Nanostructures

In Situ Assembly of Zeolitic Building Blocks into High-Order Structures**

Gang Hu, Ding Ma, Lin Liu, Mojie Cheng, and Xinhe Bao**

The construction of inorganic architectures with hierarchically complex structures and optimized properties for specific applications is a current objective in materials chemistry.[1–3] These highly organized materials, including metal and metal oxides,[4] bio-minerals,[5] and micro- and mesoporous materials,[6–9] have great potential as agents in medical (e.g. controlled drug delivery), optical, electronic, and magnetic applications. Besides methods that involve molecular cross-linking[10] or antibody–antigen recognition,[11] most high order inorganic frameworks are synthesized through so-called template-assisted processes with building blocks such as nanosized particles generated either beforehand or in situ.

Although classified under template-assisted processes, many different approaches are involved in such constructions. Examples include guided growth within confined geometries,[12] monodisperse polymer sphere templating,[5b,6b,7,13] polydimethylsilane stamp patterning,[4c,8] aligned polyurethane film matrixing,[9] and pseudomorphic self-templating transformations.[14] Interestingly, although different in concept, most templates employed in the synthesis are hard templates such as polymer spheres, organic moulds, macro- or mesoporous materials,[15] bacteria,[6a] and diatom shells.[16] Very few cases of simple processes that employ soft or dual-soft templates to build complex multilevel structures from a functional basic unit have been reported. Herein we describe a feasible and facile one-pot approach, which first employs a small HMI (hexamethyleneimine) template to generate the sheetlike building block of microporous MCM-22 zeolite, then a supramolecular surfactant acts as a co-template to assist the assembly of these building blocks in situ into superstructures.

[*] G. Hu, Dr. D. Ma, L. Liu, Prof. M. Cheng, Prof. X. Bao
State Key Laboratory of Catalysis
Dalian Institute of Chemical Physics
Chinese Academy of Sciences
Dalian 116023 (China)
Fax: (+86) 411-8469-4447
E-mail: xhbao@dicp.ac.cn
Dr. D. Ma
School of Chemistry, University of Bristol
Bristol, BS8 1TS (UK)
Fax: (+44) 117-9290-509
E-mail: ding.ma@bristol.ac.uk

[**] Financial support (2003CB615806, G1999022406) from the National Natural Science Foundation and the Ministry of Science and Technology of the People's Republic of China is gratefully acknowledged. We also thank Dr. M. Li and Dr. D. Walsh for kind help in composing the paper and Dr. A. Kulak for technical expertise.

Supporting information for this article is available on the WWW under http://www.angewandte.org or from the author.

Zeolite MCM-22 is a microporous material composed of interconnected $\{4^3 5^6 6^3 [4^3]\}$ building units that form two independent pore systems: two-dimensional 10-ring intralayer channels, and 12-ring interlayer supercages with depths of 18.2 Å, both of which are accessible through 10-ring apertures.[17] This makes MCM-22 a promising catalyst for many processes and particularly for hydrocarbon conversion reactions.[18] Although other morphologies such as spheres have been reported for MCM-22 crystals,[19] the more common morphology of MCM-22 consists of sheetlike discs or aggregates of several cross-linked discs of 2–5 μm in diameter and 10–40 nm in thickness (see Supporting Information).[20,21]

However, when nonionic surfactants were added to the system doughnutlike products with different morphologies and surface patterns were obtained. For example, the sample M20 was synthesized with the addition of $C_{16}H_{33}(OC_2H_4)_{20}OH$ at 160 °C. The dominant product (> 85 % yield) was spherical with a diameter of around 8–10 μm and with a scaled surface pattern (Figure 1 a, b).

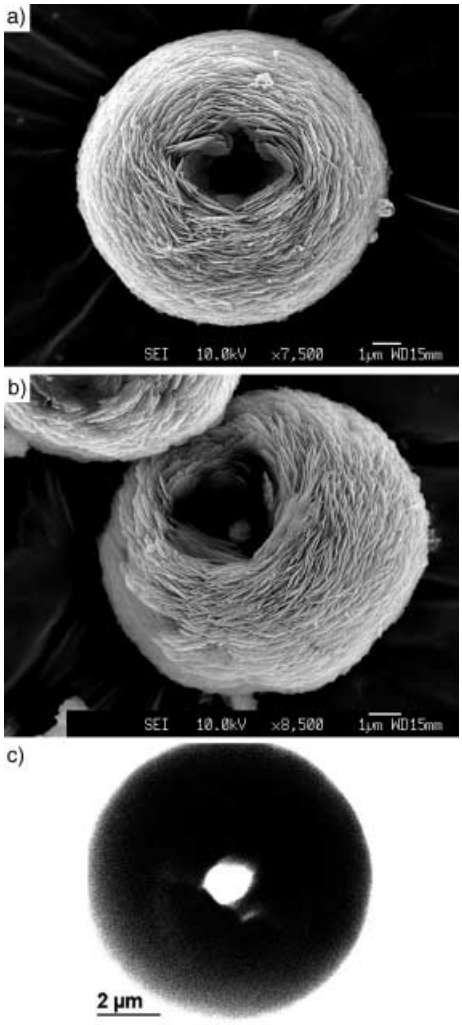

Figure 1. a), b) FESEM pictures, and c) TEM picture of the sample M20 (synthesized at 160 °C in the presence of $C_{16}H_{33}(OC_2H_4)_{20}OH$). Scale-like patterns and holes can be observed on the spheres in a) and b); c) shows a channel penetrating the sphere.

  DOI: 10.1002/ange.200453777

Furthermore, small holes (≈1.5–2 μm according to TEM) were found at the center of the spherical structures. The TEM image of the top surface of one such particle (Figure 1c) revealed that these holes are actually channels that penetrate through the centers of the particles to form doughnutlike structures. FESEM (field emission scanning electron microscopy) measurements of samples prepared in the absence of nonionic surfactants show that the doughnuts are composed of individual sheets (see Supporting Information). However, at this stage, we were unable to conclude whether or not these scales consisted of MCM-22 as the influence of the added nonionic surfactants on the crystal structure of the products was unclear.

XRD studies of the "doughnuts" before and after calcination (Figure 2a, I and II, respectively) reveal both sharp and broad peaks that are consistent with the diffraction peaks of zeolite MCM-22.[17,20] Peaks at $2\theta = 6.5$ and 7.2° in Figure 2aI corresponding to (002) and (100) peaks, respectively, are clearly discerned. After calcination, these two peaks overlap owing to the structural contraction along the *c* axis. Furthermore, broad peaks within the range 18–25° split and become more defined (Figure 2aII). These XRD details are characteristic of MCM-22 and confirm that the building blocks constructing the giant doughnut-shaped structures are indeed zeolite MCM-22. The nonionic surfactants, which are not involved in the crystallization process of the individual scales of MCM-22 sheets, are instead involved in the self-assembly into super-structures. Importantly, samples prepared in the absence of nonionic surfactants consist of normal random oriented MCM-22 discs (see Supporting Information).

Figure 2bI shows the ^{13}C cross-polarization/magic-angle spinning (CP/MAS) NMR spectrum of the sample MN (which was synthesized in the absence of surfactant). When compared with the standard ^{13}C NMR spectrum of HMI which displays three signals at $\delta = 51.5$, 34, and 29.5 ppm (see Supporting Information), the three peaks in the spectrum of MN at $\delta \approx 55$, 47, and 26.5 ppm can be assigned to signals arising from C1, C1, and C2/C3 (Figure 2b), respectively, of HMI molecules within the zeolitic channels.[21] The two signals for C1 are attributed to HMI template molecules residing in two distinct inter- and intralayer void spaces of MCM-22; the strong interactions between HMI molecules and the zeolite framework account for the different chemical shifts for C1.[21]

Two additional peaks appear in the NMR spectrum of the sample M20 (synthesized in the presence of surfactant), one at $\delta \approx 28$ ppm and the other at $\delta \approx 53.5$ ppm (Figure 2bII) although the sample was repeatedly washed with deionized water before NMR measurements. When compared with the ^{13}C NMR spectrum of the surfactant $C_{16}H_{33}(OC_2H_4)_{20}OH$ (see Supporting Information), we see that the signal at $\delta =$ 28 ppm in Figure 2bII arises from the carbon atoms in the alkyl chain $C_{16}H_{33}$-, whereas the signal at $\delta \approx 53.5$ ppm can be assigned to the carbon atoms in the oxyethylene groups $(OC_2H_4)_{20}$. The former peak overlaps with that of the C2/C3 atoms of HMI to result in a more intense peak at $\delta \approx 28$ ppm. The shift in the signals arising from pure surfactant molecules and those incorporated into the MCM-22 superstructure are

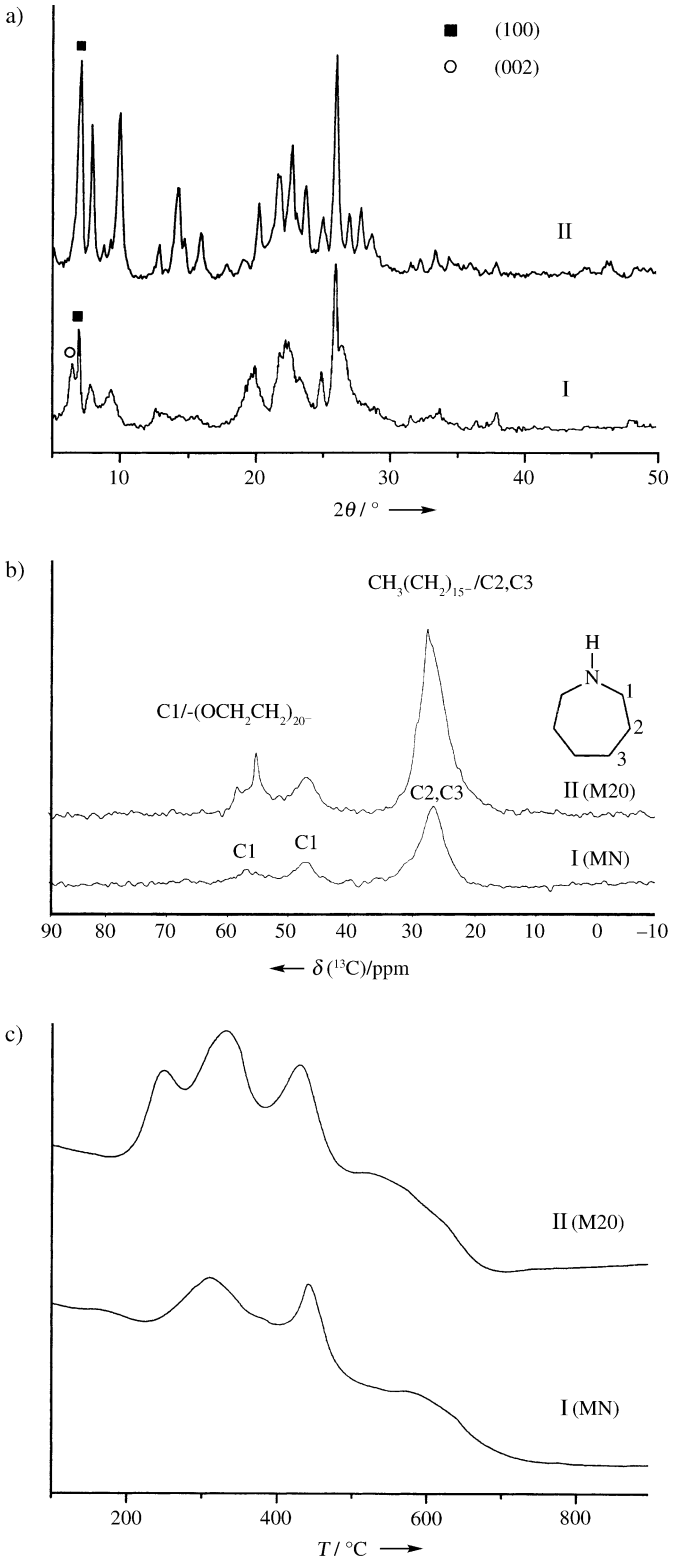

Figure 2. a) XRD patterns of sample M20: I) before and II) after calcination. The disappearance of the (002) peak and the increased intensity of the peaks at 18–28° are characteristic of the zeolite MCM-22; b) ^{13}C CP/MAS NMR spectra: I) MN (prepared in the absence of surfactant) and II) M20; the signal from incorporated oxyethylene groups is seen at $\delta = 53.5$ ppm; (c) DTA curves of synthesized samples I) MN and II) M20; the new peak at about 250 °C arises from oxyethylene carbon species.

again attributed to strong interactions of the nonionic surfactant with the MCM-22 discs. This result suggests that the nonionic surfactant remains between the adjacent discs of individual MCM-22 discs and contributes to the assembly of the MCM-22 sheets into the "doughnuts". In other words, the strong interactions between the surfactant molecules and MCM-22 building-block discs are the driving force for the formation of the zeolitic superstructure.

To determine whether the nonionic surfactant had taken part in the assembly of the doughnutlike superstructure, further investigations by DTA (differential thermal analysis) were undertaken as shown in Figure 2c. For the standard MCM-22 sample, the weight loss in the range of 220–520 °C is mainly attributed to the removal of the organic template HMI from the framework.[21] Two peaks were observed when MN (the sample prepared without the addition of surfactants) was analyzed; these peaks arise from the presence of template HMI molecules (Figure 2c I) inside the zeolitic channels. For sample M20, the peak at about 250 °C on the DTA curve (Figure 2c II) is characteristic of the removal of oxyethylene carbon species. Again, this confirms that the second template (i.e. the surfactant $C_{16}H_{33}(OC_2H_4)_{20}OH$) does participate in the assembly of MCM-22 discs to form high-order superstructures.

An investigation throughout the duration of the growing process aided us in understanding the assembly mechanism of the doughnutlike superstructures. After the gelation of slurrylike reactants (normally after 2–3 days in a hydrothermal bomb at 160 °C), partially crystallized intermediates, which are occasionally found as by-products (about 5-20%) in the final product, were sometimes observed (see Supporting Information). These intermediates are thin, oriented MCM-22 discs aggregated together which then form rolls probably owing to the larger surface tension on the side with nonionic surfactant micelles. This stress imbalance probably arises from the strong interaction between MCM-22 crystallites and surfactant micelles.

A clearer description of this process is illustrated in Scheme 1. In a typical synthetic procedure for MCM-22, the mixture of $NaAlO_2$, H_2O, HMI, and silica sol produces a milky slurry. With further hydrothermal reaction, single or aggregated MCM-22 discs with MWW topology crystallize from the system. If a nonionic surfactant (e.g. $C_{16}H_{33}(OC_2H_4)_{20}OH$) is added to the slurry with vigorous stirring before the hydrothermal crystallization process, a synergic effect of HMI and $C_{16}H_{33}(OC_2H_4)_{20}OH$ combines both the growth of MCM-22 discs and the self-assembly in situ of disclike MCM-22 building blocks in a one-pot reaction. However, the presence of a possible intermediate state of the product suggests that the formation of the doughnutlike superstructure through the growth of MCM-22 discs and the assembly of these zeolitic building blocks is likely to occur by a sequential process instead of a one-step procedure. Under these conditions, the formation of doughnutlike structures is probably geometrically more favorable than the normal flat discs.

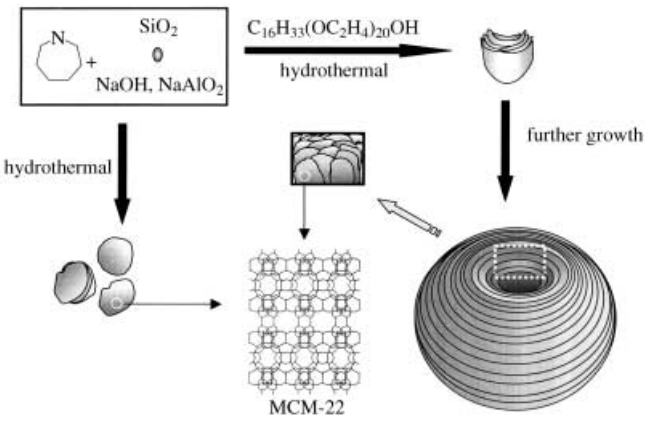

Scheme 1. With the addition of nonionic surfactant, rolled MCM-22 building blocks crystallize in the system and assemble in situ into doughnutlike superstructures. Without the addition of surfactant, MCM-22 discs do not form macrostructured spherical products.

During the study, we also noticed that products with different morphologies could be obtained upon variation of the crystallization temperature. Taking M20 for example, when the system was heated at 150 °C uniform spherical superstructures were synthesized with an average diameter of 8–12 μm (see Supporting Information). XRD analysis confirmed that the superstructures consisted of building blocks with MWW topology (MCM-22). However, high resolution SEM pictures show that the MCM-22 discs assembled in a much more compact manner at 150 °C (Figure 3a) than at 160 °C (Figure 3b).

Besides $C_{16}H_{33}(OC_2H_4)_{20}OH$, other nonionic surfactants such as $C_{16}H_{33}(OC_2H_4)_{10}OH$ and $H(OC_2H_4)_{20}(OC_3H_6)_{70}(OC_2H_4)_{20}OH$ (P123) that have different numbers of oxyethylene groups as well as different molecular sizes were employed in the synthesis. SEM pictures show remarkable morphological differences of the two samples obtained at 150 °C when compared with that of M20. The surface of the M10 superstructure (prepared in the presence of $C_{16}H_{33}(OC_2H_4)_{10}OH$) was more coarse and scale-like fragments on the surfaces were observed among the particles (Figure 3c). Sample MP (with the addition of P123) consisted of spheres with a similar average diameter of about 8–12 μm. However, Figure 3e shows that the linear patterns on the MP surfaces are thicker and more compact than those on the M10 and M20 surfaces. When the crystallization temperatures were increased to 160 °C, a much less compact assembly was observed by SEM analysis of samples M10 (Figure 3d) and MP (Figure 3f). For $C_{16}H_{33}(OC_2H_4)_{10}OH$, which has a smaller polyoxyethylene group, the MCM-22 discs were only poorly aggregated and no doughnutlike superstructures were observed by SEM for the sample synthesized at 160 °C (Figure 3d). However, in this case a peony-like superstructure resulted in which there was no penetrating hole in the center. Owing to the larger polyoxyethylene groups in P123 and $C_{16}H_{33}(OC_2H_4)_{20}OH$, the interactions between nanoscale MCM-22 building blocks and surfactant molecules (in the *z* direction) were still strong enough for the discs to assemble into large spherical superstructures, though in a relatively less compact manner at 160 °C. XRD results of samples M10 and MP at 150 and 160 °C both confirmed that these products were still constructed of zeolite MCM-22. ^{13}C CP/MAS NMR and DTA studies gave similar results for M20.

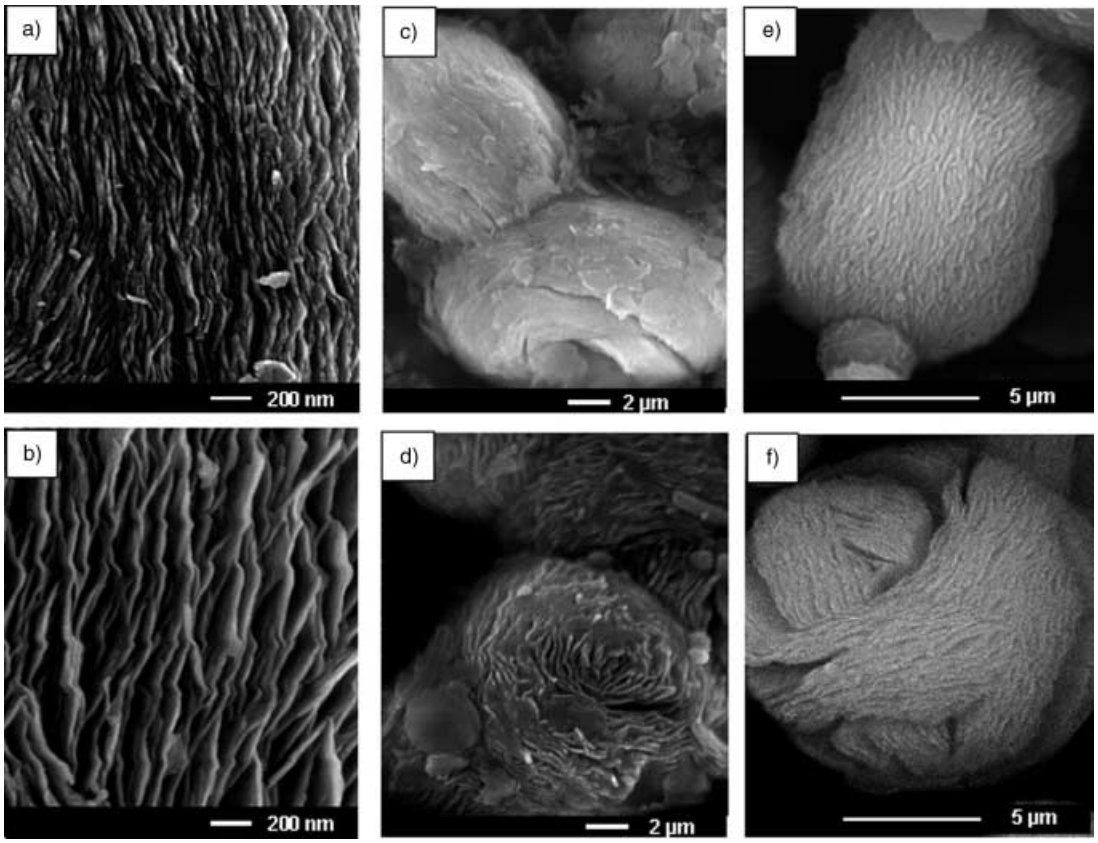

Figure 3. FESEM pictures of samples synthesized with different surfactants at different temperatures. a), c), and e) show samples M20, M10, and MP, respectively, at 150 °C; b), d), and f) are SEM pictures of the respective samples crystallized at 160 °C. The MCM-22 building blocks are arranged in a more compact manner at lower temperature and with increasing numbers of oxyethylene groups.

It is likely that the repeating oxyethylene units in the surfactant molecules play an important role in the assembly process. The interactions of these hydrophilic groups with the aluminosilicates appear to be the driving force behind the assembly of the zeolitic units into superstructures. With more hydrophilic oxyethylene units in the surfactant molecules, the interactions become stronger and so the zeolitic discs are assembled more tightly. This is possibly the reason why MP superstructures have more compact surface linear patterns than those of M20 and M10 superstructures. It is not quite clear why the discs combined less compactly with increased reaction temperatures, but a possible explanation is that higher temperatures are not favorable for the surfactants to form "liquid-crystal" micelles in the mixture and thus the capacity of the surfactants to assemble is weakened. Another factor may be that the polyoxyethylene chains in nonionic surfactant molecules are not stable and decompose at higher temperatures, which might also account for the less compact arrangement of the discs in the samples obtained at higher temperatures.

In conclusion, we have shown that high-order superstructures with nanoscale zeolitic building units can be synthesized through the synergic dual-template method by a one-pot reaction, which opens a new way to construct hierarchical macrostructures using functional inorganic units as building blocks.

Experimental Section

Reagents were used as received without further purification: silica sol (25 wt %), hexamethyleneimine (HMI), sodium aluminate, sodium hydroxide, deionized water and nonionic surfactants. Three nonionic surfactants were used: $C_{16}H_{33}(OC_2H_4)_{10}OH$, $C_{16}H_{33}(OC_2H_4)_{20}OH$, and $H(OC_2H_4)_{20}(OC_3H_6)_{70}(OC_2H_4)_{20}OH$ (P123). A typical synthetic procedure for different MCM-22 samples follows:

Sodium aluminate (1 g) and sodium hydroxide (0.2 g) were dissolved in deionized water (135 mL), and HMI (10.3 g) was added dropwise to the stirred mixture. Then, either $C_{16}H_{33}(OC_2H_4)_{20}OH$ (1.0 g) or $C_{16}H_{33}(OC_2H_4)_{10}OH$ (1.0 g) or P123 (2.0 g) was dissolved in silica sol (100.2 g) and added to the above mixture with vigorous stirring. After stirring for 5 h at room temperature, the slurry was transferred into a stainless-steel hydrothermal bomb lined with teflon and heated at 150 °C or 160 °C for 4–6 days. The final products (labeled M20, M10, and MP, respectively) were washed repeatedly with cold and hot deionized water and then dried at 80 °C. Calcination of the synthesized products was carried out in air at 540 °C for 10 h. For comparison, a normal MCM-22 sample (MN) was also synthesized in the same way but without the addition of surfactant. The products were characterized by X-ray powder diffraction (XRD, Rigaku Dmax/rb diffractometer with $Cu_{K\alpha}$ radiation, $\lambda = 0.1542$ nm, 40 kV, 100 mA), electron microscopy (Hitachi HB600 and JEOL 6300F FEGSEM), nuclear magnetic resonance spectroscopy (NMR, Bruker DRX-400 with BBO MAS probe and 4-mm ZrO_2 rotors; ^{13}C CP/MAS NMR spectra were recorded at 100.62 MHz with a 2500-μs contact time, a 4-s recycle delay, and a 4-kHz spinning rate), and differential thermal analysis (DTA, Perkin-Elmer DTA1700) studies.

Received: January 19, 2004 [Z53777]

Keywords: nanostructures · self-assembly · surfactants · template synthesis · zeolites

[1] S. Mann, G. A. Ozin, *Nature* **1996**, *382*, 313.
[2] I. Dierking, *Adv. Mater.* **2003**, *15*, 152.
[3] A. Stein, *Adv. Mater.* **2003**, *15*, 763.
[4] a) O. D. Velev, P. M. Tessier, A. M. Lenhoff, E. W. Kaler, *Nature* **1999**, *401*, 548; b) A. Imhof, D. J. Pine, *Nature* **1997**, *389*, 948; c) P. Yang, T. Deng, D. Zhao, P. Feng, D. Pine, B. F. Chmelka, G. M. Whitesides, G. D. Stucky, *Science* **1998**, *282*, 2244; d) Z. Yang, Z. Niu, Y. Lu, Z. Hu, C. C. Han, *Angew. Chem.* **2003**, *115*, 1987; *Angew. Chem. Int. Ed.* **2003**, *42*, 1943.
[5] a) W. Shenton, D. Pum, U. B. Sleytr, S. Mann, *Nature* **1997**, *389*, 585; b) B. T. Holland, C. F. Blanford, A. Stein, *Science* **1998**, *281*, 538.
[6] a) S. A. Davis, S. L Burkett, N. H. Mendeison, S. Mann, *Nature* **1997**, *385*, 420; b) K. H. Rhodes, S. A. Davis, F. Caruso, B. Zhang, S. Mann, *Chem. Mater.* **2000**, *12*, 2832.
[7] B. T. Holland, L. Abrams, A. Stein, *J. Am. Chem. Soc.* **1999**, *121*, 4308.
[8] L. Huang, Z. Wang, J. Sun, L. Miao, Q. Li, Y. Yan, D. Zhao, *J. Am. Chem. Soc.* **2000**, *122*, 3530.
[9] J. S. Lee, Y. J. Lee, E. L. Tae, Y. S. Park, K. B. Yoon, *Science* **2003**, *301*, 818.
[10] R. P. Andres, J. D. Bielefeld, J. I. Henderson, D. B. Janes, V. R. Kolagunta, C. P. Kubiak, W. Mahoney, R. G. Osifchin, *Science* **1996**, *273*, 1690.
[11] W. Shenton, S. A. Davis, S. Mann, *Adv. Mater.* **1999**, *11*, 449.
[12] M. Trau, N. Yao, E. Kim, Y. Xia, G. M. Whitesides, I. A. Aksay, *Nature* **1997**, *390*, 694.
[13] X. D. Wang, W. L. Yang, Y. Tang, Y. J. Wang, S. K. Fu, Z. Gao, *Chem. Commun.* **2000**, 2161; A. Dong, Y. Wang, Y. Tang, Y. Zhang, N. Ren, Z. Gao, *Adv. Mater.* **2002**, *14*, 1506.
[14] T. Martin, A. Galarneau, F. Di Renzo, F. Fajula, D. Plee, *Angew. Chem.* **2002**, *114*, 2702; *Angew. Chem. Int. Ed.* **2002**, *41*, 2590.
[15] C. Z. Yu, J. Fan, B. Z. Tian, D. Y. Zhao, *Adv. Mater.* **2002**, *14*, 1742.
[16] M. W. Anderson, S. M. Holmes, N. Hanif, C. S. Cundy, *Angew. Chem.* **2000**, *112*, 2819; *Angew. Chem. Int. Ed.* **2000**, *39*, 2707.
[17] M. E. Leonowicz, J. A. Lawton, S. L. Lawton, M. K. Rubin, *Science* **1994**, *264*, 1910; G. J. Kennedy, S. L. Lawton, M. K. Rubin, *J. Am. Chem. Soc.* **1994**, *116*, 11 000; S. L. Lawton, M. E. Leonowicz, R. D. Partridge, P. Chu, M. E. Rubin, *Microporous Mesoporous Mater.* **1998**, *23*, 109.
[18] D. Ma, Y. Shu, X. Han, X. liu, Y. Xu, X. Bao, *J. Phys. Chem. B* **2001**, *105*, 1170.
[19] a) A. Marques, J. Monteiro, H. O. Pastore, *Microporous Mesoporous Mater.* **1999**, *32*, 131; b) M. Cheng, G. Hu, D. Tan, X. Bao, *Microporous Mesoporous Mater.* **2001**, *50*, 69; c) A. Corma, C. Corell, J. Perez-Pariente, *Zeolites* **1995**, *15*, 2. Attempts to repeat the experiments reported in reference [19a] yield only disclike products (see Supporting Information) instead of the spherical products reported. In other works,[19c] some spherical MCM-22 aggregates were occasionally observed, although the main products were small thin plates. To the best of our knowledge, no other relevant work had ever been reported before. An inadvertent introduction of organic materials into the system may have led to the false phenomena in the above reports and the poor reproducibility encountered afterwards.
[20] a) I. Mochida, S. Eguchi, M. Hironaka, S. Nagao, K. Sakanishi, D. D. Whitehurst, *Zeolites* **1997**, *18*, 142; b) I. Güray, J. Warzywoda, N. Baç, A. Sacco, Jr., *Microporous Mesoporous Mater.* **1999**, *31*, 241.
[21] S. L. Lawton, A. S. Fung, G. J. Kennedy, L. B. Alemany, C. D. Chang, G. H. Hatzikos, D. N. Lissy, M. K. Rubin, H.-K. C. Timken, S. Steuernagel, D. E. Wossner, *J. Phys. Chem.* **1996**, *100*, 3788.

